

Coil Efficiency for Inductive Peripheral Nerve Stimulation

Philipp Braun¹, Jonathan Rapp¹, Werner Hemmert¹, and Bernhard Gleich¹

Abstract—Magnetic stimulation of peripheral nerves is evoked by electric field gradients caused by high-intensity, pulsed magnetic fields created from a coil. Currents required for stimulation are very high, therefore devices are large, expensive, and often too complex for many applications like rehabilitation therapy. For repetitive stimulation, coil heating due to power loss poses a further limitation. The geometry of the magnetic coil determines field depth and focality, making it the most important factor that determines the current required for neuronal excitation. However, the comparison between different coil geometries is difficult and depends on the specific application. Especially the distance between nerve and coil plays a crucial role. In this investigation, the electric field distribution of 14 different coil geometries was calculated for a typical peripheral nerve stimulation with a 27 mm distance between axon and coil. Coil parameters like field strength and focality were determined with electromagnetic field simulations. In a second analysis, the activating function along the axon was calculated, which quantifies the efficiency of neuronal stimulation. Moreover, coil designs were evaluated concerning power efficacy based on ohmic losses. Our results indicate that power efficacy of magnetic neurostimulation can be improved significantly by up to 40% with optimized coil designs.

Index Terms—Coil design, magnetic stimulation, field simulation, peripheral stimulation.

I. INTRODUCTION

TRANSCRANIAL magnetic stimulation (TMS) is already established for various diagnostic and therapeutic treatments [1], [2], and most stimulation devices and coils are optimized for this application [3]–[6]. A drawback of magnetic nerve stimulation are the high voltages and currents, which require large stimulation devices and coils. These devices are not energy efficient and heating of the stimulation coils becomes a problem when repetitive stimulation is required.

Manuscript received 12 January 2022; revised 9 May 2022 and 14 June 2022; accepted 13 July 2022. Date of publication 20 July 2022; date of current version 5 August 2022. This work was supported by the German Research Foundation under Grant DFG 398820493. (Philipp Braun and Jonathan Rapp contributed equally to this work.) (Corresponding author: Jonathan Rapp.)

Philipp Braun is with the Klinikum rechts der Isar (MRI), Technische Universität München, 81675 München, Germany (e-mail: philipp21.braun@tum.de).

Jonathan Rapp and Bernhard Gleich are with the Munich Institute of Biomedical Engineering (MIBE), Technische Universität München, 85748 Garching, Germany (e-mail: jonathan.rapp@tum.de).

Werner Hemmert is with the Bio-inspired Information Processing (BAI), Munich Institute of Biomedical Engineering (MIBE), Technische Universität München, 85748 Garching, Germany.

This article has supplementary downloadable material available at <https://doi.org/10.1109/TNSRE.2022.3192761>, provided by the authors.

Digital Object Identifier 10.1109/TNSRE.2022.3192761

In this respect, the application-specific optimization of the stimulation coils is crucial: if the efficiency of the nerve stimulation was improved, this would directly entail lower stimulation currents and voltages, smaller devices with better energy efficiency, and less heating of the coils.

Requirements of the magnetic coil for peripheral nerve stimulation are of increasing interest, especially for applications in rehabilitation therapy [7]–[9]. Due to recent developments, public attention has been drawn to respiratory diseases, which might increase the demand for therapy methods concerning lung functionality. Peripheral magnetic stimulation is a promising technique for such treatments, in particular the excitation of the phrenic nerve [10]–[14]. Stimulation of the phrenic nerve at the neck has the potential to train the diaphragm and avoid ventilator-induced diaphragm dysfunction [15]–[17]. An established tool to activate or restore muscle function is electric stimulation. Compared to those therapies, which use electrodes to deliver the required electric field, magnetic stimulation benefits from being non-invasive and contactless. This maximizes patient comfort and also eliminates risks from potential surgical interventions. Another advantage compared to electric stimulation is the relatively uniform distribution of magnetic permeability in the tissue, which makes it possible to control the magnetic field distribution precisely [18]. However, one large disadvantage comes from the fact that a considerably higher amount of energy is required for magnetic stimulation, therefore devices are large and expensive. Reducing the required energy would allow a broader field of applications for magnetic stimulation. Precise adjustments of all stimulation parameters are required [2], and the coil geometry is an essential aspect.

To reach this goal, large effort has already been put into the investigation of coil geometries and optimizing field distributions for TMS, as it is the most prominent area for magnetic stimulation [3]–[5], [19], [20]. For TMS, field focality plays a crucial role, since the stimulation of nearby tissue can yield critical side effects. Many authors have evaluated the influence of coil design on focal magnetic stimulation, but they mostly focused on the electric field strength and focality [6], [21]–[25]. However, peripheral nerve stimulation has different requirements than TMS. First, in contrast to the central nervous system, the stimulus does not have to overcome the periencephalic layers, which reduce the required electromagnetic field significantly [1]. Second, motor neurons are larger and hence, easier to be stimulated than axons in the brain [26], [27]. A crucial limitation for therapeutical applications is the requirement of repetitive pulses [28]. Together with current strength, the frequency of repetitive stimulation deter-

mines coil heating and thus, affecting treatment time or cooling requirements. Focality, in terms of peripheral stimulation, depends on the specific application. Whereas a focal field might be an advantage in some cases to avoid the stimulation of nearby tissue, a broad field might be desired to easier find the target nerve in other cases. Therefore, for the use of magnetic stimulation in peripheral rehabilitation applications, focality and field strength might not have the highest priority. Instead, reducing the energy and more compact devices are more achievable and relevant for therapy. Some techniques for optimized coil design have been proposed, including the use of iron cores or boundary elements method [29]–[31]. These methods are generic and can be applied to most coil designs. However, a comprehensive coil comparison considering field efficiency and power efficacy has not been done so far.

In this work, we consider (1) the field efficiency and (2) the power efficacy based on ohmic losses. First, we calculated the spatial field distribution for all coils with the same coil current, and compared the field efficiency using the activating function (AF) along an axon [32], [33]. Second, we scaled the coil current such, that all coils achieved the same AF amplitude. Based on that coil current, the power efficacy of each coil was determined using the ohmic losses.

The analyzed coil geometries are based on either already commercially available coils such as the Figure-Of-8 coil (*FO8*) or *Single Coil* [34], include slight modifications, or were proposed by other researchers. The *Slinky-3* and *3D Differential* coil were proposed by Cret *et al.* [21] and the modified *FO8* is based on the work of Kato *et al.* [22], [23]. The cornered coils are based on the work of Fang *et al.* [35]. In general, only idealized coil geometries will be discussed, which do not include the wiring to the external current supply. However, for some coil geometries both a “realistic” as well as a more “ideal” structure will be introduced. This allows to compare the results of both to verify the general use of idealized shapes, thus, reducing computation time significantly. All of the proposed coil configurations aim to either increase field focality, field strength, or both at the cost of wire length. The optimal configuration must be chosen such that the energy requirement is minimal and yet the desired nerve stimulation is achieved.

II. METHODS

Different coil geometries produce different spatial distributions of the electric field. We evaluated the resulting electric fields according to the stimulation strength and the focality. The stimulation strength is related to the spatial derivative of the electric field and is quantified by the AF along the target axon [32]. Field focality is based on the spread of the electric field. To relate the field efficiency to the power efficacy, we compared the ohmic losses based on the AF. This allows the discussion of the stimulation efficacy of each coil geometry.

A. Analyzed Coil Geometries

The electric field data is generated using CST Studio Suite (Dassault Systèmes Simulia), a computational electromagnetics tool, that uses the finite-element method, the finite

integration technique and the transmission-line matrix method to provide efficient and effective solvers for the Maxwell equations. In particular, Ampère’s law and the Maxwell-Faraday equation are employed to calculate the electric field based on the coil current. CST’s calculations of the electromagnetic field are based on Maxwell’s grid equation approach. We used CST’s low frequency magnetoquasistatic solver, which is suitable for problems in areas significantly smaller than the wavelength. The boundary box had a size of $400 \times 400 \times 100$ mm in x , y and z direction, which was large compared to the dimensions of the coil ($\approx 200 \times 100 \times 7$ mm). The axon to calculate the AF is running in y -direction at $x = 0$ and the coils are placed at a distance $z = 27$ mm in the xy -plane. The transverse electric field at the boundary was set to zero, assuming that it was far enough for any relevant contribution. The material inside the boundary box was saline solution.

The analyzed coil geometries are shown in Figure 1. Models of *Single Coil*, *FO8* and *Two FO8* were implemented twice, one idealized and one realistic version (Figure 1a and 1b, 1e and 1f, 1m and 1n). Realistic coil models consisted of only one single wire, whereas the other coil geometries were modelled with several independent wire segments. The realistic versions imitate an external power supply, which produces the desired shape of the current. The use of realistic structures allows to obtain more realistic electric field distributions as well as a more precise calculation of the ohmic losses. However, it comes at the expense of higher computational time as well as the possible emergence of undesirable artefacts in the spatial distribution of the electric field. Hence, the difference between the results of realistic and ideal coils will be shortly discussed in order to justify the simplification. All coils are wired in a single layer, except the *Two FO8s* coils, where two coils are stacked, and the *Slinky-3*, *3D Differential* and *Bent Solenoid*, which include tilted coils. The spacing between the stacked coils is 25 mm and the distance between coil and axon refers to the closest point of the coil to the axon.

The current in each coil segment is given by $I(t) = I_0 \cdot \sin(2\pi f t)$, with a frequency of $f = 10$ kHz and a peak current $I_0 = 6$ kA. These are typical parameters for magnetic stimulation [4], [20], [36]. A frequency of 10 kHz corresponds to a pulse length of 100 μ s for biphasic pulses, which is shorter than the pulses of most available stimulator types. Nevertheless, a shorter pulse length requires less threshold current and is more efficient, whereas a pulse length of 100 μ s is still in the feasible range of device development [37]. Higher frequencies in the coil lead to increasing relevance of skin effect and proximity effect and therefore, the choice of the conductor material plays a crucial role. In this work, we assume the conductor in the coil to be a high-frequency litz wire. Since the single wires in high frequency litzes are thin enough, increasing resistance due to skin and proximity effect are negligible [38]. Higher efficiency for litz wire compared to solid copper has been shown by [39], [40].

A rectangular wire with a cross-section of 7 mm \times 3 mm was used for each proposed coil configuration. The wire was made of high frequency copper litz wire. High frequency litz wire includes insulation layers and air between the single strands,

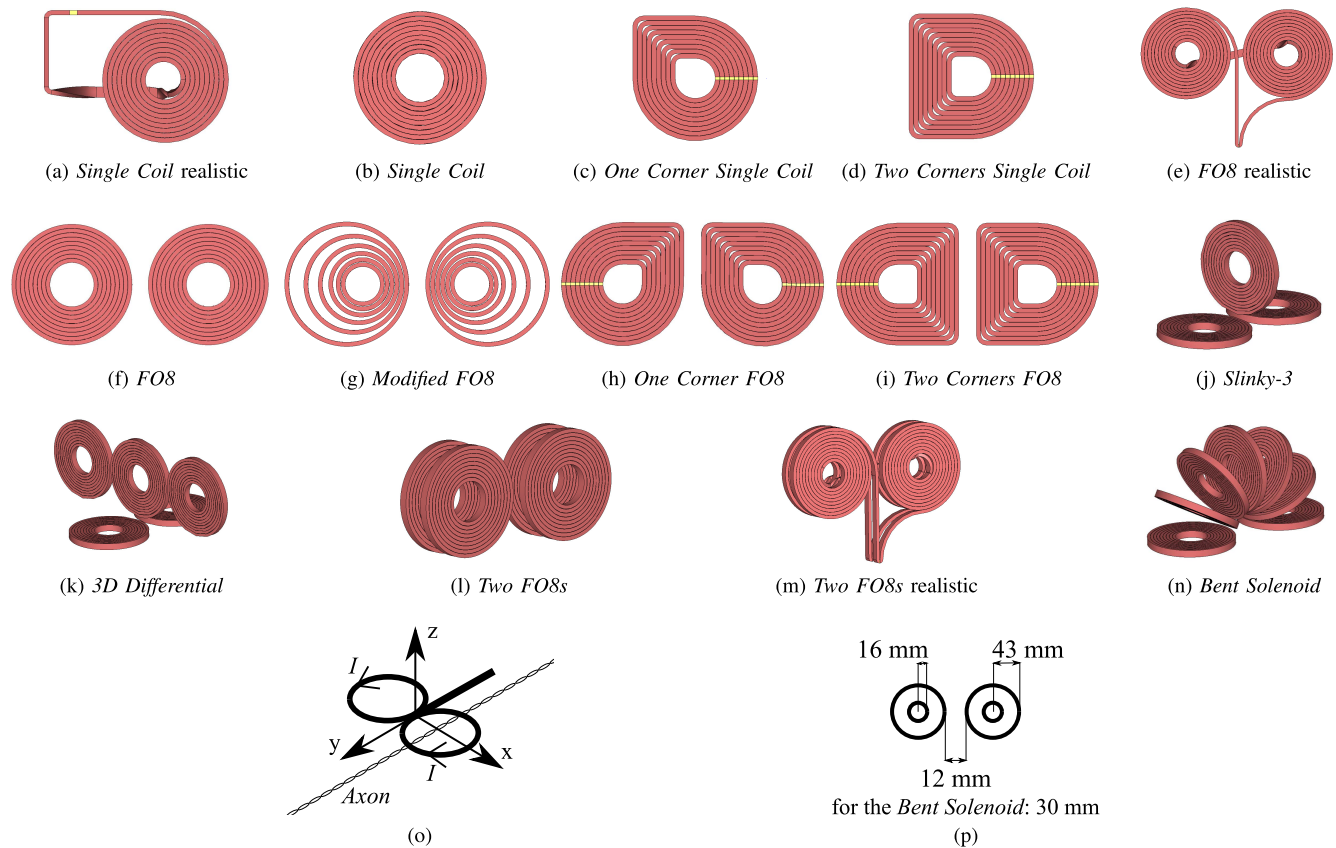


Fig. 1. Tested coil geometries; realistic structures refer to a more realistic wiring geometry, which imitates an external current source; (o) Coordinate system in relation to coil; (p) Dimensions of the coils; Further information about the coils and the axon position can be found in Figure S1 in the supplementary material.

reducing the percentage of conducting copper. Typically, the copper fill factor is between 65% and 80% (e.g. RUPALIT Profile, Rudolf Pack GmbH & Co. KG, Gummersbach, Germany). Without loss of generality, we assume a copper fill factor of 72.5% (average fill factor) resulting in a conductivity for the wire $\sigma = 4.2 \cdot 10^7 \frac{S}{m}$ (to be scaled for other copper fill factors). The outermost radius for one coil segment was set to 43 mm (Figure 1p). The distance between two coils in a plane was 12 mm except for the *Bent Solenoid* geometry, where it was 30 mm. Each of the considered coils had $N = 9$ windings spaced 0.15 mm apart from each other.

Within this work, we have compared single coils (Figure 1b,1c,1d), multi-coil arrangements (1f,1h,1i,1j,1k, 1l,1n) and a modified version of the *FO8* (1g) with tighter winding in the coil center. The latter one is discussed separately, as its wire length is shorter having only $N = 6$ windings. To allow a comparison between *FO8* and *Modified FO8*, an additional *FO8* model with only $N = 6$ instead of $N = 9$ windings was created. For the multi-coil arrangements, the coils were connected in series as pictured in Figure 1e. All coil segments were driven with the same current and the current density was assumed constant across the wire cross section. In all multi-coil arrangements, the current in the single coils ran in the same direction at the center of the coil, which causes the field to add up to a large focal peak. For *FO8*-like coils, that means that the current in both coils was in opposing

direction. One exception was the *3D Differential*, where the current in the three coils perpendicular to the *FO8* ran in the same direction.

B. Field Focality

Field focality describes the spread of the electric field and can be defined by the full-width-half-maximum (FWHM). Within this work, we were specifically interested in the spread of E_y in x -direction, which determines the offset a coil may have in relation to the target nerve. Since we consider a straight nerve, the focality in this work is mostly a measure for selective stimulation, i.e., about how much surrounding tissue is stimulated. Therefore, we use a one-dimensional focality, which is the width between the two points in x -direction where the field has decayed to half of its maximum. Focality is measured over x at $y = 0$, for different coil distances z_0 . Large FWHM values indicate weak focality. For single coils, the FWHM is calculated over both peaks, as they are equally able to stimulate the axon.

C. Field Efficiency

The field efficiency describes the ability to stimulate a nerve based on the current in the coil. A good measure for that purpose is the AF at the target nerve site, which evaluates the required stimulation strength on neuronal systems based

on the spatial field gradients [32], [33], [41]. The AF is calculated along a hypothetical axon of 300 mm length at a distance of $z_0 = 27$ mm from the coil. The axon runs along the y -axis at $x = 0$. We assumed the axon to be straight which fairly represents peripheral motor axons within a given stimulation site. To calculate the AF, we used the approach of quasipotentials which are derived from the external parallel electric field [42], [43]. We sampled the field values at distinct points along the axon, separated by the spacing \vec{s} and representing the nodes of Ranvier. For a motor axon of 12.8 μm diameter the spacing \vec{s} between the nodes is 1349 μm and the node length is 1 μm [27].

The quasipotentials ϕ were acquired from the electric field volume box calculated in CST by

$$\phi_i = \phi_{i-1} - \int \vec{E} \cdot d\vec{s} \approx \phi_{i-1} - \frac{1}{2}(\vec{E}_i + \vec{E}_{i-1}) \cdot \vec{s}, \quad (1)$$

where \vec{E} denotes the electric field at the axon location and \vec{s} describes the position vector between two nodes of Ranvier i and $i-1$. Only the electric field component parallel to the axon is taken into account for this calculation. Similar approaches were used by Wang *et al.*, who used precise theoretical and computational models to confirm this assumption [42].

The AF is subsequently acquired from the quasipotential given by

$$\text{AF} = \frac{\phi_{i-1} - 2\phi_i + \phi_{i+1}}{s^2}, \quad (2)$$

where i numerates the nodes of Ranvier, ϕ is the electric potential along the axon and s is the distance between neighboring Nodes of Ranvier [32]. A positive AF corresponds to a depolarization of the axon membrane, which can create an action potential, when it reaches a certain threshold. A negative AF causes a hyperpolarization of the axon membrane, which cannot cause an action potential [32], although it could block a propagating action potential. Such a case has to be considered in simulations and experiments including the temporal field shape, especially for repetitive stimulation. However, since we are using a sinusoidal current inside the magnetic coil, the electric field will oscillate with a cosine shape causing an alternating sign of the AF. Hence, a positive AF will become negative during the sinusoidal period and vice versa, so the value of interest is the absolute AF. Due to the action potential being relayed to both sides of the axon, it is sufficient for only one node of Ranvier to trigger an action potential, as it will then propagate along the whole axon.

The AF identifies positions along the axon which are likely to be stimulated based on the spatial electric field distribution. Nevertheless, the AF alone does not determine neuronal firing threshold, as it also depends on the temporal field shape, as well as neuronal parameters as myelin thickness, fiber thickness and distance between Nodes of Ranvier [41]. However, for the purpose of comparing coil geometries and field shapes, the AF is appropriate.

D. Power Efficacy

In section II-C we described how much field gradient can be achieved for a certain current value. For further analysis,

the required coil current is scaled such that all coils achieve the same AF amplitude. Subsequently, ohmic losses were calculated for the scaled coil current and how much power was dissipated in heat. This indicates how much power was lost in each coil for the same activation ability and is referred to as power efficacy.

The resistance of a wire segment is given by

$$R = \rho \frac{L}{A}, \quad (3)$$

where ρ denotes the specific resistivity, L is the length of the coil wire and A the area of the rectangular wire cross section given by 7 mm \times 3 mm. The ohmic losses can then be calculated using

$$P_{\text{real}} = R \cdot I_{\text{RMS}}^2, \quad (4)$$

with I_{RMS} being the root mean square of the AC current. Ohmic loss is the power that dissipates due to heating. In magnetic stimulation, it is reasonable to state this power in units of Joules per pulse. In our simulations, we consider a biphasic pulse of 10 kHz which corresponds to a pulse duration of 100 μs .

To scale the coil current, the AF amplitude of the *Single Coil* with a peak current of 6 kA was used as reference. Due to the direct proportionality of the coil current and the electric field and hence, also the AF, an increase of the AF by a factor of two would also require increasing the coil current by a factor of two. This change in coil current would then cause a change in the resulting ohmic losses given by Equation 4. Additional ohmic losses occur in the tissue at the stimulation site and in the connection to the stimulation device. These losses depend on the specific application and are not considered within this work.

III. RESULTS

The electric field was calculated for each proposed coil geometry and evaluated using the AF along a linear axon segment. To compare different coil geometries, the efficiency of stimulation is described by the relation between stimulation strength and the occurring heating of the magnetic coil due to the ohmic losses. In the following, only the idealized coil shapes are evaluated according to the approach described in section II-C. The comparison between real and idealized coil geometries is shown in Figure S2 and S3 of the supplementary material. We found that idealized coil geometries yield similar results and hence, the use of simplified structures is justified.

A. Electric Field Calculations

Calculated electrical field shapes for each coil geometry are given in Figure S1 of the supplementary material. The use of multi-coil arrangements, geometries consisting of more than a single coil, allows for a strong focal peak along the central axis of the coil plane. This is due to superposition of the electric field from each individual coil segment. However, as the actual stimulation strength is only based on the AF, given by the gradient along axon direction, these results do not indicate yet, that single coils yield considerably worse results.

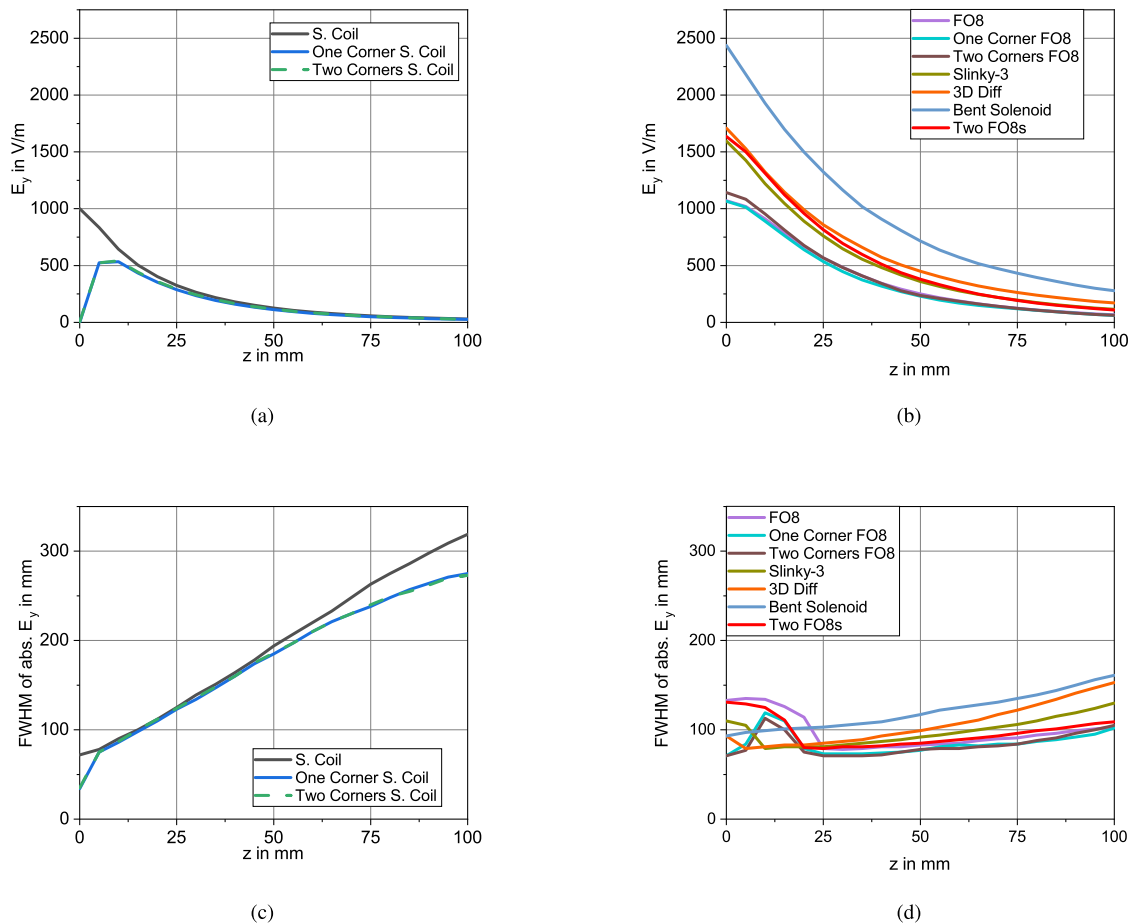


Fig. 2. Maximum absolute field intensity of E_y in the xy -plane over coil distance z_0 for (a) single coils and (b) multi-coil arrangements; FWHM of E_y over coil distance z_0 (c) single coils and (d) multi-coil arrangements; In (a) and (c) the data of the *One Corner Single Coil* and the *Two Corner Single Coil* are almost identical and thus, overlapping. The FWHM is measured over x at $y = 0$. Field irregularities, observable in (d) at distances $z_0 < 25$ or in (a) and (b) at $z_0 < 10$, are due to non-perfect coil meshes and do not represent valid data.

B. Focality

Figure 2 shows the maximum absolute E_y in the xy -plane for different coil distances z_0 . Coils with several coil segments showed stronger field intensities, due to the superposition of the distinct field distributions. The *Bent Solenoid* (Figure 1n) had the largest field intensity (2.5 kV m^{-1} directly at the coil), followed by *3D Differential* (Figure 1k, 1.7 kV m^{-1}), the *Two FO8* and the *Slinky-3* (Figure 1l and 1j, both 1.6 kV m^{-1}). The *Two Corners FO8* (Figure 1i) and the *FO8* (Figure 1f) showed a similar field intensity (both 1.2 kV m^{-1}). The *Single Coil* (Figure 1b) had a maximum of 1 kV m^{-1} and the single coils with corner showed similar behavior. The FWHM (Full-Width-Half-Maximum) is measured over x at $y = 0$, shown in Figure 2. Compared to multi-coil configurations, the single coils showed a higher increase of FWHM with coil distance. There is hardly any difference in field magnitude and FWHM between the *One Corner Single Coil* and the *Two Corner Single Coil*, the data in Figure 2 is almost overlapping. In general, coils involving a cornered design showed slightly less FWHM and have thus higher focality. The *Bent Solenoid* had the worst FWHM at a coil distance of 27 mm (105 mm), followed by *3D Differential* (87 mm) and *Slinky-3* (83 mm).

For coil distances smaller than 20 mm, we observed strong irregularities in the FWHM, which can be seen in Figure 2d.

Similar distortions were observed for E_y and FWHM calculations for single coils with corner, shown in Figure 2a and 2c. Those irregularities are caused by the non-perfect mesh of the coil. It affects the area close to the coil mesh which we consider as acceptable, since we are interested in distances of $z_0 > 20$ mm.

C. Field Efficiency

Figure 3 shows the AF at $x = 0$ for multi-coil configurations and at $x = 40$ mm for single coils, which is tangential to the coil wire. For single coils, the AF is highest for axon positions directly below the wire (at $x = 40$ mm). For multi-coil arrangements, the optimal axon position is at $x = 0$, where the field peaks of the individual coils overlap. An exemplary axon is pictured in Figure S1 of the supplementary material to mark the position of the axon for single coil and multi-coil arrangements. Multi-coil arrangements produce a strong focal peak where the single coils of the structure are overlapping or close to each other. Thus, the highest AF magnitude can be achieved when the axon runs between the two coils. Further, the absolute AF calculated for varying x -positions of the axon is depicted, showing how the AF changes with a coil offset in x -direction. The plots indicate that the *Bent Solenoid* achieved the highest stimulation strength to the axon across

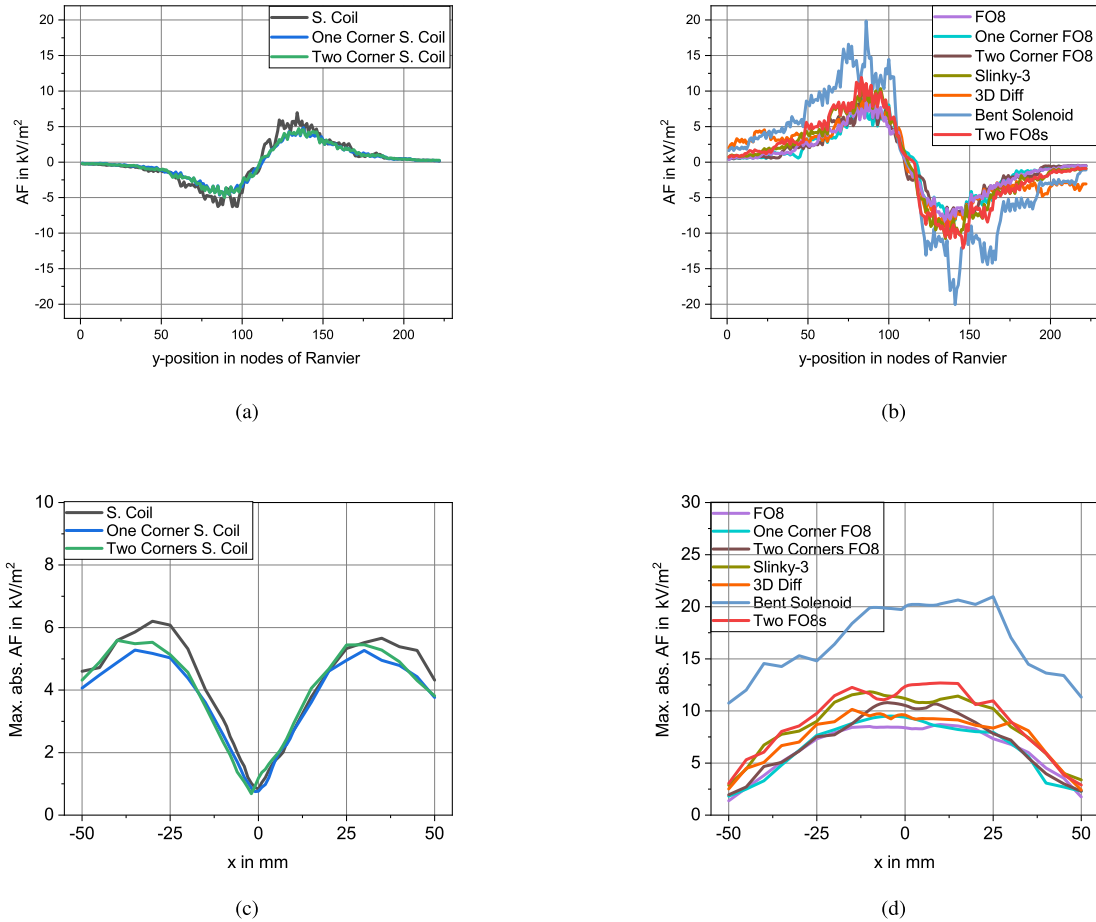


Fig. 3. The AF along the axon is shown for (a) single coils and (b) geometries consisting of multiple coil segments. The axon runs from $y = -150$ mm to $+150$ mm at a coil distance of $z_0 = 27$ mm. For single coils, the axon is placed at $x = 40$ mm and for multi-coil configurations at $x = 0$. The x -axis enumerates the nodes of Ranvier with a spacing of 1.349 mm. (c) and (d) show the maximum of the AF for different x -positions of the axon.

all x -positions. Compared to multi-coil configurations, single coils seem to provide much worse results, while also causing a much broader spread of the electric field.

In general, coils that achieved a high electric field amplitude also had higher AF values. The *3D Differential* had a similar field amplitude as *Slinky-3* and *Two FO8s* but lower AF amplitude. *FO8*, *One Corner FO8* and *Two Corner FO8* had clearly lower field values but just slightly lower AF amplitudes. Compared to the single coils with corner, the round single coil had higher AF values. However, the field of the single coil was not symmetric, which is due to irregularities in the field distribution. Those irregularities become more prominent when calculating the spatial gradient, as the AF does. Similar asymmetries can be observed for the *Bent Solenoid* or the *Slinky-3*.

A comparison between the results of idealized and realistic coil shapes, shown in Figure S2 and S3 of the supplementary material, indicated small changes in the AF between both representations (by $< 15\%$), the field distribution in space was very similar. Realistic shapes seem to produce unrealistic field artifacts due to insufficient accuracy in calculating electric field gradients.

The comparison between the *FO8* and the modified *FO8* showed that both coils had a similar performance.

D. Ohmic Losses

The ohmic losses for a peak coil current of 6 kA are given in Table I. Complex coil structures require a longer wires and thus, have higher losses. In the further analysis, the peak coil current for each individual coil configuration was not fixed any more, but was varied to achieve the same AF as the *SingleCoil* with a peak current of 6 kA. Based on that current, ohmic losses for each coil configuration were calculated, which can be used to estimate the general stimulation efficiency of different coil shapes. Ohmic losses for 6 kA and scaled currents are shown in Table I.

For 6 kA, the *Bent Solenoid* had the highest ohmic losses, whereas it provided the most efficient stimulation when the AF is considered. Therefore, it would require the lowest coil current. Compared to the standard round *FO8*, ohmic losses were reduced by 40%. Similarly, *FO8s* where the midsection was modified to have corners as well as the *Slinky-3* coil, seem to perform at a roughly 20% higher efficiency compared to the standard round *FO8*. The round *Single Coil* had a similar energy efficiency as the round *FO8*. However, the other single coils analyzed in this work seem to perform much worse than every other geometry. The *3D Differential* had the worst efficiency. It requires a long wire, while the maximum achievable AF was relatively low.

TABLE I
OHMIC LOSSES AND AF

Magnetic Coil	Ohmic loss at 6 kA J Pulse	Max. AF kV m ²	Scaling factor	Scaled ohmic loss J Pulse
<i>S. Coil</i>	3.24	6.20	1.00	3.24
<i>One Corner S. Coil</i>	3.34	5.28	1.17	4.60
<i>Two Corners S. Coil</i>	3.81	5.59	1.11	4.68
<i>FO8</i>	6.47	8.70	0.71	3.29
<i>One Corner FO8</i>	6.68	9.50	0.65	2.85
<i>Two Corners FO8</i>	7.62	10.80	0.57	2.51
<i>Slinky-3</i>	9.70	11.8	0.53	2.68
<i>3D Differential</i>	16.19	10.20	0.61	5.98
<i>Bent Solenoid</i>	22.66	21.00	0.30	1.98
<i>Two FO8s</i>	12.95	12.7	0.49	3.09

Ohmic losses for a peak coil current of 6 kA; Maximum achieved AF at 6 kA; Scaling factor for coil current to achieve the same AF for all coils; Scaled ohmic losses for the scaled coil current; These new scaled ohmic losses represent the energy efficiency of individual coil geometries to achieve a given stimulation effect.

At fixed AF, the *Modified FO8* showed 20% less ohmic losses than the *FO8* with 6 windings, indicating significantly higher effectiveness (ohmic loss: 3.77J per pulse and 4.91J per pulse, respectively).

IV. DISCUSSION

Limitations for magnetic stimulation are huge and expensive devices and in case of repetitive stimulation in therapeutical applications, coil heating. While the first issue is addressed by optimizing field efficiency, the latter one is due to ohmic losses and requires an optimization concerning power efficacy. Field efficiency describes the electric field generated by a certain coil current and voltage and determines the specifications for the power semiconductors and capacitors in the device. In case of peripheral stimulation, field efficiency can be quantified by the AF of a straight axon, which evaluates the field gradients [33], [41]–[44]. Several approaches have been proposed to optimize the field efficiency of coils, such as coils with high permeability cores [30], [31], improved winding patterns [6], [45], [46], boundary element methods [47] and coil position or winding layers [44]. For repetitive stimulation, coil heating is a critical problem [48], [49]. It determines how much output power is required and occurs due to the ohmic losses in the coil. Some techniques to reduce coil heating have been proposed, for example coil cooling, heat sinks or iron cores [49], [50]. Different coil geometries were compared concerning field efficiency, depth and focality [6], [21]–[25], [51]. However, authors either focused on field efficiency and focality or coil heating. This work is a comprehensive comparison of commonly discussed coil designs, considering field strength and focality, neuronal activation and power efficacy. Hence, we first calculated the AF based on the spatial field distribution induced by a coil current of 6 kA. In the second analysis, the coil current was scaled such that all coils achieved the same AF amplitude. Based on the scaled coil current, we calculated the power dissipation due to ohmic losses. This method relates field efficiency to the ohmic losses. Our results outline which coil geometries optimize the electric field with minimum coil heating.

A. Coil Comparison

A good coil would provide a high field with a small current and still not require too much wire. Coil geometries which consist of several coils, like the *Bent Solenoid* or the *Two FO8s* generate high fields, but also have high ohmic losses. The goal is to find a good trade-off between those two measures.

Our analysis showed that at the same peak current, large coils like the *Bent Solenoid* or *Slinky-3* generate high field intensities, at the cost of focality. A trade-off between depth and focality has already been shown by Deng *et al.* [3]. Single coils showed low focality, since they simultaneously produce equally negative and positive peaks, and the FWHM was calculated over both. However, in peripheral nerve stimulation both cases might be of interest. Coils with high focality can avoid the stimulation of nearby fascicles within a nerve or nearby nerves, whereas coils with a high field spread make it easier to hit the target nerve.

The ability of coils to stimulate an axon was quantified by the AF. A similar approach from Davids *et al.* [41] showed similar values. Both, AF and field intensity, were highest for the *Bent Solenoid*. The *FO8* and its variations with corners had the lowest field intensity compared to other multi-coil structures, whereas the AF values were rather similar to the other coils. They also require relatively low amounts of wire and thus, have low ohmic losses, which is a good trade-off between field efficiency and power efficacy. *FO8* geometries with corners had even better results. While the field intensity was similar to one of the *FO8*, their AF values were higher. Since ohmic losses are small, the scaled ohmic loss showed that corners in *FO8* structures yield efficacy improvements of up to 20%.

In contrast, the *3D Differential* coil generates a higher field intensity than the *FO8* structures, similar to the one of *Two FO8s* and *Slinky-3*, but has lower AF values than the latter ones. A reason are the three coils which are aligned on top along the axon direction. This arrangement smears the electric field and thus, flattens the spatial field gradient. In combination with the long wire in the whole coil structure, ohmic losses lead to a bad efficacy.

The *Two FO8s* geometry provides a relatively high field intensity and higher AF than most other coils. Still, the scaled ohmic losses show that the long wire reduces its efficacy and makes it slightly worse than the normal *FO8*. The *Slinky-3* geometry has similar field intensity and AF values, but consists of only three coils instead of four, which makes it better than the *Two FO8s* also the *FO8* and *One Corner FO8*.

Both, efficiency and efficacy were the highest for the *Bent solenoid*. It had the highest ohmic losses as well, but the field efficiency is high enough to operate it with such low currents that ohmic losses are still better than for all other coils.

Single coils have worse results when compared to multi-coil geometries, which is the result of having only one coil segment contributing to the stimulation of the axon, while multi-coil structures generate superimposed fields. Some applications however, might benefit from the broad electric field [25].

The *Bent Solenoid* had the best power efficacy. Compared to the standard round *FO8*, ohmic losses can be reduced by 40% and the coil current by roughly 58%. However, this comes at

the price of weight and size, as the *Bent Solenoid* consists of seven coils. Apart from high costs, this is a major disadvantage in everyday use and practicability. *FO8s*, where the midsection has been modified to have corners, as well as the *Slinky-3* coil, seem to perform at a roughly 20% higher efficiency compared to the standard round *FO8*. They also have slightly lower current requirements. With their much lower size and weight, they may prove to be a good alternative to the nowadays used round *FO8* or the proposed *Bent Solenoid* structure. The *Two Corners FO8* in particular has the advantage of having roughly the same size and weight as the regular *FO8*. This makes the replacement of currently commercially available *FO8* coils very simple. The *Modified FO8* proved to increase the efficiency as well, however it is limited by the number of windings. Without increasing the general coil size, more than six windings are hardly feasible. A more detailed trade-off evaluation may be required for specific applications. The round *Single Coil* performs at roughly the same energy efficiency as the round *FO8*. However, the other single coils analyzed in this investigation perform worse than every other geometry. Their higher current requirements are another significant disadvantage compared to multi-coil configurations. The predictions of this study can easily be tested in a clinical setting. The stimulation coil can be easily changed in a stimulation device and can lead to a significant reduction of energy consumption as well as heating.

B. Limitations

Comparing different coils in experimental setups is challenging and complex. Sophisticated setups are required and the field characteristics depend on the hardware of the stimulation device, mainly the inductance of the coil and the capacitance of the pulse capacitor. Hence, simulations are a helpful tool for comprehensive coil comparisons. Nevertheless, this work is of purely theoretical nature, the simulations are based on several assumptions. Using the AF as an indicator for neuronal stimulation is suitable for the analysis of spatial field distributions on peripheral axons, as it relies on the spatial field gradient. However, to determine whether an axon is stimulated, many more parameters must be considered, including the temporal field shape and the axon size and structure itself. Our field calculations are only valid for high-frequency litz wire, which is commonly used by manufacturers. Coils of a solid wire will have significantly higher ohmic losses due to skin and proximity effects. Another limitation of this work is that the fields were calculated for saline solution. This is a good method to quantitatively compare the spatial field distribution. However, the electric field amplitude will be attenuated for a volume conductor model. To calculate a more realistic field distribution, an anatomical volume model for the desired stimulation site is required.

C. Conclusion

We conclude that the *Bent Solenoid* (Figure 1n) seems to be most efficient coil when stimulation focality, weight and size are not crucial. For other applications, the cornered *FO8* (1i) appears to provide better results than the round

FO8 (Figure 1f) used in clinical applications today and should be considered as an alternative. The relevance of focality needs to be evaluated according to the specific application and the potential presence of surrounding nerve fibers. The optimization of the magnetic coil is a relatively simple modification, which nevertheless provides large benefits. First, the optimized coils can be tested with commercially available stimulation devices. We have shown that there is significant room for improvements in specific application areas, where the stimulation efficiency can be increased. This improvement immediately reduces stimulation voltage, current and energy of the stimulation device, which means that their size can be reduced. The higher energy efficiency also reduces coil heating, which is essential for sustained stimulation sequences. With these new devices, new clinical applications will become possible.

REFERENCES

- [1] P. M. Rossini *et al.*, "Non-invasive electrical and magnetic stimulation of the brain, spinal cord, roots and peripheral nerves: Basic principles and procedures for routine clinical and research application. An updated report from an I.F.C.N. Committee," *Clin. Neurophysiol., J. Int. Fed. Clin. Neurophysiol.*, vol. 126, no. 6, pp. 1071–1107, Jun. 2015.
- [2] H.-J. Park, G. Bonmassar, J. A. Kaltenbach, A. G. Machado, N. F. Manzoor, and J. T. Gale, "Activation of the central nervous system induced by micro-magnetic stimulation," *Nature Commun.*, vol. 4, no. 1, p. 2463, Dec. 2013.
- [3] Z. D. Deng, S. H. Lisanby, and A. V. Peterchev, "Electric field depth-focality tradeoff in transcranial magnetic stimulation: Simulation comparison of 50 coil designs," *Brain Stimulation*, vol. 6, no. 1, pp. 1–13, 2013.
- [4] L. M. Koponen, J. O. Nieminen, and R. J. Ilmoniemi, "Minimum-energy coils for transcranial magnetic stimulation: Application to focal stimulation," *Brain Stimulation*, vol. 8, no. 1, pp. 124–134, Jan. 2015.
- [5] F. S. Salinas, J. L. Lancaster, and P. T. Fox, "Detailed 3D models of the induced electric field of transcranial magnetic stimulation coils," *Phys. Med. Biol.*, vol. 52, no. 10, pp. 2879–2892, May 2007.
- [6] L. G. Cohen *et al.*, "Effects of coil design on delivery of focal magnetic stimulation. Technical considerations," *Electroencephalogr. Clin. Neurophysiol.*, vol. 75, no. 4, pp. 350–357, Apr. 1990.
- [7] C. Carrico, K. C. Chelette, P. M. Westgate, E. Salmon-Powell, L. Nichols, and L. Sawaki, "Randomized trial of peripheral nerve stimulation to enhance modified constraint-induced therapy after stroke," *Amer. J. Phys. Med. Rehabil.*, vol. 95, no. 6, pp. 397–406, 2016.
- [8] P. Celnik, N.-J. Paik, Y. Vandermeeren, M. Dimyan, and L. G. Cohen, "Effects of combined peripheral nerve stimulation and brain polarization on performance of a motor sequence task after chronic stroke," *Stroke*, vol. 40, no. 5, pp. 1764–1771, May 2009.
- [9] C. Krewer, S. Hartl, F. Müller, and E. Koenig, "Effects of repetitive peripheral magnetic stimulation on upper-limb spasticity and impairment in patients with spastic hemiparesis: A randomized, double-blind, sham-controlled study," *Arch. Phys. Med. Rehabil.*, vol. 95, no. 6, pp. 1039–1047, Jun. 2014.
- [10] W. W. L. Glenn, W. G. Holcomb, R. K. Shaw, J. F. Hogan, and K. R. Holschuh, "Long-term ventilatory support by diaphragm pacing in quadriplegia," *Ann. Surgery*, vol. 183, no. 5, pp. 566–577, May 1976.
- [11] C. H. Hamnegard *et al.*, "Mouth pressure in response to magnetic stimulation of the phrenic nerves.," *Thorax*, vol. 50, no. 6, pp. 620–624, Jun. 1995.
- [12] G. H. Mills, D. Kyroussis, C. H. Hamnegard, S. Wragg, J. Moxham, and M. Green, "Unilateral magnetic stimulation of the phrenic nerve.," *Thorax*, vol. 50, no. 11, pp. 1162–1172, Nov. 1995.
- [13] T. Similowski, S. Mehiri, A. Duguet, V. Attali, C. Straus, and J.-P. Derenne, "Comparison of magnetic and electrical phrenic nerve stimulation in assessment of phrenic nerve conduction time," *J. Appl. Physiol.*, vol. 82, no. 4, pp. 1190–1199, Apr. 1997.
- [14] S. Wragg *et al.*, "Comparison of cervical magnetic stimulation and bilateral percutaneous electrical stimulation of the phrenic nerves in normal subjects," *Eur. Respiratory J.*, vol. 7, no. 10, pp. 1788–1792, Oct. 1994.

- [15] B. Ahn *et al.*, “Phrenic nerve stimulation increases human diaphragm fiber force after cardiothoracic surgery,” *Amer. J. Respiratory Crit. Care Med.*, vol. 190, no. 7, pp. 837–839, Oct. 2014.
- [16] H. Masmoudi *et al.*, “Can phrenic stimulation protect the diaphragm from mechanical ventilation-induced damage?” *Eur. Respiratory J.*, vol. 42, no. 1, pp. 280–283, Jul. 2013.
- [17] A. D. Martin *et al.*, “Effect of intermittent phrenic nerve stimulation during cardiothoracic surgery on mitochondrial respiration in the human diaphragm,” *Crit. Care Med.*, vol. 42, no. 2, p. e152, 2014.
- [18] P. Kosta, D. J. Warren, and G. Lazzi, “Selective stimulation of rat sciatic nerve using an array of mm-size magnetic coils: A simulation study,” *Healthcare Technol. Lett.*, vol. 6, no. 3, pp. 70–75, Jun. 2019.
- [19] M. Lu and S. Ueno, “Comparison of the induced fields using different coil configurations during deep transcranial magnetic stimulation,” *PLoS ONE*, vol. 12, no. 6, Jun. 2017, Art. no. e0178422.
- [20] P. Rastogi, E. G. Lee, R. L. Hadimani, and D. C. Jiles, “Transcranial magnetic stimulation-coil design with improved focality,” *AIP Adv.*, vol. 7, no. 5, May 2017, Art. no. 056705.
- [21] L. Cret, M. Plesa, D. D. Micu, and R. V. Ciupa, “Magnetic coils design for focal stimulation of the nervous system,” in *Proc. IEEE EUROCON*, Piscataway, NJ, USA, Sep. 2007, pp. 1998–2003.
- [22] T. Kato, M. Sekino, T. Matsuzaki, A. Nishikawa, Y. Saitoh, and H. Ohsaki, “Fabrication of a prototype magnetic stimulator equipped with eccentric spiral coils,” in *Proc. Annu. Int. Conf. IEEE Eng. Med. Biol. Soc.*, Aug. 2011, pp. 1985–1988.
- [23] M. Sekino *et al.*, “Eccentric figure-eight coils for transcranial magnetic stimulation,” *Bioelectromagnetics*, vol. 36, no. 1, pp. 55–65, Jan. 2015.
- [24] C. Bischoff, H. Riescher, J. Machetanz, B.-U. Meyer, and B. Conrad, “Comparison of various coils used for magnetic stimulation of peripheral motor nerves: Physiological considerations and consequences for diagnostic use,” *Electroencephalogr. Clin. Neurophysiol./Electromyography Motor Control*, vol. 97, no. 6, pp. 332–340, Dec. 1995.
- [25] S. M. Goetz, H.-G. Herzog, N. Gatteringer, and B. Gleich, “Comparison of coil designs for peripheral magnetic muscle stimulation,” *J. Neural Eng.*, vol. 8, no. 5, Oct. 2011, Art. no. 056007.
- [26] R. Klinke, H.-C. Pape, A. Kurtz, and S. Silbernagl, *Physiologie* (Thieme Electronic Book Library), 6th ed. 2010. [Online]. Available: <https://eref.thieme.de/ebooks/2109863>
- [27] C. C. McIntyre, A. G. Richardson, and W. M. Grill, “Modeling the excitability of mammalian nerve fibers: Influence of afterpotentials on the recovery cycle,” *J. Neurophysiol.*, vol. 87, no. 2, pp. 995–1006, Feb. 2002.
- [28] W. Klomjai, R. Katz, and A. Lackmy-Vallée, “Basic principles of transcranial magnetic stimulation (TMS) and repetitive TMS (rTMS),” *Ann. Phys. Rehabil. Med.*, vol. 58, no. 4, pp. 208–213, Sep. 2015.
- [29] C. C. Sánchez, F. J. García-Pacheco, J. M. G. Rodríguez, and J. R. Hill, “An inverse boundary element method computational framework for designing optimal TMS coils,” *Eng. Anal. Boundary Elements*, vol. 88, pp. 156–169, Mar. 2018.
- [30] R. Carbanaru and D. M. Durand, “Toroidal coil models for transcutaneous magnetic stimulation of nerves,” *IEEE Trans. Biomed. Eng.*, vol. 48, no. 4, pp. 434–441, Apr. 2001.
- [31] R. Salvador, P. C. Miranda, Y. Roth, and A. Zangen, “High-permeability core coils for transcranial magnetic stimulation of deep brain regions,” in *Proc. 29th Annu. Int. Conf. IEEE Eng. Med. Biol. Soc.*, Aug. 2007, pp. 6653–6656.
- [32] F. Rattay, “Analysis of models for extracellular fiber stimulation,” *IEEE Trans. Biomed. Eng.*, vol. 36, no. 7, pp. 676–682, Jul. 1989.
- [33] E. J. Peterson, O. Izad, and D. J. Tyler, “Predicting myelinated axon activation using spatial characteristics of the extracellular field,” *J. Neural Eng.*, vol. 8, no. 4, Aug. 2011, Art. no. 046030.
- [34] P. J. Maccabee, L. Eberle, V. E. Amassian, R. Q. Cracco, and A. Rudell, “Spatial distribution of the electric field induced in volume by round and figure ‘8’ magnetic coils: Relevance to activation of sensory nerve fibers,” *Electroencephalogr. Clin. Neurophysiol.*, vol. 76, no. 2, pp. 131–141, Aug. 1990.
- [35] X. Fang, H. Ding, C. Liu, J. Shao, Z. He, and Y. Huang, “Transcranial magnetic stimulation: U-shaped coil design for improved intracranial induced electrical field,” *AIP Adv.*, vol. 10, no. 3, Mar. 2020, Art. no. 035131.
- [36] M. T. Rubens and T. P. Zanto, “Parameterization of transcranial magnetic stimulation,” *J. Neurophysiol.*, vol. 107, no. 5, pp. 1257–1259, Mar. 2012.
- [37] J. Rapp, P. Braun, W. Hemmert, and B. Gleich, “Optimal pulse configuration for peripheral inductive nerve stimulation,” *Biomed. Phys. Eng. Exp.*, vol. 8, no. 2, Mar. 2022, Art. no. 025020.
- [38] M. Hallett and S. Chokroverty, *Magnetic Stimulation in Clinical Neurophysiology*, 2nd ed. Philadelphia, Pennsylvania: Elsevier, 2005.
- [39] M. Talebinejad, S. Musallam, and A. E. Marble, “A transcranial magnetic stimulation coil using rectangular braided Litz wire,” in *Proc. IEEE Int. Symp. Med. Meas. Appl.*, May 2011, pp. 280–283.
- [40] L. M. Koponen, S. M. Goetz, and A. V. Peterchev, “Double-containment coil with enhanced winding mounting for transcranial magnetic stimulation with reduced acoustic noise,” *IEEE Trans. Biomed. Eng.*, vol. 68, no. 7, pp. 2233–2240, Jul. 2021.
- [41] M. Davids, B. Guérin, V. Klein, M. Schmelz, L. R. Schad, and L. L. Wald, “Optimizing selective stimulation of peripheral nerves with arrays of coils or surface electrodes using a linear peripheral nerve stimulation metric,” *J. Neural Eng.*, vol. 17, no. 1, Jan. 2020, Art. no. 016029.
- [42] B. Wang, W. M. Grill, and A. V. Peterchev, “Coupling magnetically induced electric fields to neurons: Longitudinal and transverse activation,” *Biophys. J.*, vol. 115, no. 1, pp. 95–107, Jul. 2018.
- [43] A. S. Aberra, B. Wang, W. M. Grill, and A. V. Peterchev, “Simulation of transcranial magnetic stimulation in head model with morphologically-realistic cortical neurons,” *Brain Stimulation*, vol. 13, no. 1, pp. 175–189, Jan. 2020.
- [44] P. Kosta, J. Mize, D. J. Warren, and G. Lazzi, “Simulation-based optimization of figure-of-eight coil designs and orientations for magnetic stimulation of peripheral nerve,” *IEEE Trans. Neural Syst. Rehabil. Eng.*, vol. 28, no. 12, pp. 2901–2913, Dec. 2020.
- [45] J. Ruohonen, P. Ravazzani, and F. Grandori, “Functional magnetic stimulation: Theory and coil optimization,” *Bioelectrochem. Bioenergetics*, vol. 47, no. 2, pp. 213–219, Dec. 1998.
- [46] K.-H. Hsu, S. S. Nagarajan, and D. M. Durand, “Analysis of efficiency of magnetic stimulation,” *IEEE Trans. Biomed. Eng.*, vol. 50, no. 11, pp. 1276–1285, Nov. 2003.
- [47] C. C. Sánchez, J. M. G. Rodríguez, Á. Q. Olozábal, and D. Blanco-Navarro, “Novel TMS coils designed using an inverse boundary element method,” *Phys. Med. Biol.*, vol. 62, no. 1, pp. 73–90, Jan. 2017.
- [48] D. Mishevich and M. Bret Schneider, “System and methods for cooling electromagnets for transcranial magnetic stimulation,” U.S. Patent 2009042863 A1, Apr. 2, 2009.
- [49] M. Belyk, B. K. Murphy, and D. S. Beal, “Accessory to dissipate heat from transcranial magnetic stimulation coils,” *J. Neurosci. Methods*, vol. 314, pp. 28–30, Feb. 2019.
- [50] C. M. Epstein and K. R. Davey, “Iron-core coils for transcranial magnetic stimulation,” *J. Clin. Neurophysiol.*, vol. 19, no. 4, pp. 376–381, Aug. 2002.
- [51] L. J. Gomez, S. M. Goetz, and A. V. Peterchev, “Design of transcranial magnetic stimulation coils with optimal trade-off between depth, focality, and energy,” *J. Neural Eng.*, vol. 15, no. 4, Aug. 2018, Art. no. 046033.